International Journal of Applied Mathematics
Volume 38 No. 3s, 2025
ISSN: 1311-1728 (printed version); ISSN: 1314-8060 (on-line version)

ENERGY EFFICIENCY ENHANCEMENT FOR SOLAR AIR HEATER BY USING CORRUGATED RIBS WITH VARIABLE HEAT FLUX FOR LAMINAR FLOW

Suha K. Jebir[1*], Mazin Y. Abdul-Kareem[2], Ahmed F. Khudheyer[3]

[1*]mechanical engineering department, engineering college, Al-Nahrain University, Baghdad, Iraq. suha.k.jebir@nahrainuniv.edu.iq
[2]Mazin Y. Abdul-Kareem, mechanical engineering department, engineering college, Al-Nahrain University, Baghdad, Iraq. mazin.y.abdulkareem@nahrainuniv.edu.iq
[3]mechanical engineering department, engineering college, Al-Nahrain University, Baghdad, Iraq. ahmed.f.khudheyer@nahrainuniv.edu.iq

Abstract

An experimental analysis is conducted to determine how corrugated absorbent tubes affect the functionality of a collector with a parabolic trough (PTC). Nine distinct helically corrugated absorbent pipes were employed for this particular purpose. Using ASHRAE standard 93 (2010) as a guide, the effects of pitch size and irregularity height upon PTC effectiveness were investigated. The range of the Re was 5000–10,000. The findings show the thermal efficiency and heat transmission. With corrugated pipes, the typical heat transfer rates rose from 85.7 to 107.2%, correlated with the pitch's percentage and irregularity height. When it equals 3 mm & 1.5 mm, respectively, the thermal efficiency reaches a maximum level of around 2.29, for both the 3 or 1.5-mm pitch size and roughness elevation respectively. In wavy pipes, the average coefficient of friction rises by 1.25 – 1.85 at certain times. Additionally, applying the most effective fit for the sequence of measurements, the changes with the Nu, as well as friction factor with pitch-to-diameter ratio, roughness, Pr, and Re, are provided as relationships.

Keywords: frictional factor; thermally effectiveness; SPTC; hexagonally curved absorber tubes.

INTRODUCTION

Heat exchangers known as trough parabolic collectors (PTCs) convert solar energy to an effective fluid, however, the heat flow surrounding the tube that absorbs energy is not uniform. Among them is a reflection that directs the flow of solar heat onto an absorber cylinder. The fluid that serves as the flowing focal line within the PTC corresponds to where the absorption tube is positioned. The tube's wall exposes the fluid to sun rays. PTCs are widely used in heating processes and steam production applications [1]. The protective coating on the outside of the tube that receives the energy [2–7] and the tracker's ability to maintain the direction of solar rays perpendicular to the outermost layer of the tube used for absorption [8–10] are two of several features that are crucial to ensuring a thermal increase of PTCs. The three primary categories for improving heat transmission in PTCs were compound, engaged, and passive techniques. The ferric chloride is used as the medium for operation and the field of magnets is applied by a force from outside via active techniques. The functioning fluid's increased conductivity to temperature improves its thermal stability [11, 12]. Using turbulent generators [13–17], porous materials [18–20], surface changes [21], various working fluid categories [22–28], and various absorber coatings [7], among other passive approaches, enhances heat transmission. Both passive as well as active approaches are used in compound procedures. Numerous research endeavors have employed passive techniques to augment the thermal efficacy of PTCs. Porous media application is one of the methods used passively to boost PTC effectiveness. Reddy et al.'s research [19] discovered that a PTC's effectiveness utilizing had the highest efficiency. The thermal effectiveness fell between 61.18 and 69.03%. A PTC containing a metallic copper foam within was assessed by Jamal-Abad et al. [18]. Around 0.5 - 90 l/h, the volume of flow varied. Because copper has a great deal of thermal conductivity, heat transfers more effectively and more quickly.

Received: July 22, 2025

ISSN: 1311-1728 (printed version); ISSN: 1314-8060 (on-line version)

Moreover, there was a roughly 45% decrease in the heat dissipation coefficient. To examine how Al2O3/oil nanofluid technology and its porous nature affect a PTC's thermal characteristics, Bozorg et al. [29] conducted a computational simulation. When the input temperature was 500 K, the pressure decreased as well as the transfer of heat coefficient rose by around 42.5% as well as 7%, accordingly. To look at how non-Newtonian tiny fluids affected a PTC's thermal efficiency, Xiong et al. [30] employed the method of the finite volume (FEM) approach. According to the findings, the friction parameter was not significantly impacted by changes in volume percentage. The empirical as well as analytical investigation was conducted by Jouybari et al. [31] to determine the effect of SiO2/water nanofluid upon a flat-plate collector's heating efficiency. According to their findings, thermal efficiency rose with They discovered that when the rate of flow grew, thermal effectiveness rose as well. In addition, as the quantity of nanoparticles rose between 0.4 - 0.6% vol, thermal performance improved by almost 1.8%. The effects of radiation including the porous design parameter regarding the thermal efficiency for a collector made of a flat plate were examined analytically by Jouybari et al. [32]. The modified Darcy model of Brinkman and Frischheimer was employed. The findings demonstrated that the irradiation parameter, rather than the overall porous form parameter, had a greater impact on the augmentation of heat transfer.

Bellos et al. [33] simulated many cylindrical longitudinally plugs in the PTC LS-2 unit in the area of turbulators' use in PTCs. PTC LS-2 component. They reported a 26.88% improvement in the thermal transfer efficiency. Using a 3-D computer simulation, Ghadirijafarbeigloo et al. [13] examined the effects of spiral louvered tapes within a PTC. The friction & Nusselt value coefficient can be increased by a maximum of 210% and 150%. According to Jaramillo et al. [34], adding a twisting tape insert to a PTC boosted its efficiency by around 3.5%. As the turning ratio increased, the heat transmission progressively reduced. The thermal effectiveness was not influenced by the twisted percentage with high Reynolds numbers. Additionally, there was a 1.5% drop in the total lost heat index and a three percent rise in the energy disposal factor. The twisted as well as nail-twisted strips were demonstrated by Jafar and Sivaraman [35] to be suitable choices for use for PTC under laminar conditions. astonishingly, thermal effectiveness rose as the tape's twist ratios decreased. It inserts were employed by Mwesigye et al. [17]; these inserts interact with the interior of the receiver's plate within a PTC. The thermal efficiency factor shifted between 0.74 - 1.27, and the frequency of entropy formation dropped by around 58%. Mwesigyet al. [36] investigated the impact of perforated plate inserts in a PTC using a thermal optimization technique. the impact of inserts with perforations in a PTC plate. Greater Reynolds numbers along with a thinner thermally boundary layer resulted from the fluid's improved thermal characteristics and decreased viscosity due to the temperature increase. Due to increasing fluid impact, the rate of heat transfer rose whilst the plate's area grew. The generation of entropy rate dropped by almost 53 percent. Bellos et al.'s research [37] showed that adding internal fins to a PTC improved its thermal performance more than employing nanofluid. They demonstrated that the best course of action for enhancing heat transport in the PTC is to employ these two techniques concurrently. Additional surface area can be obtained by applying turbulators, increasing heat transmission, but producing more substance needed.

Moreover, a PTC using turbulators saw a pressure loss that was around 500 to 2000 numerous times greater than one PTC having a simple absorber tube. However, the absorbing tube's modification of the surface had been performed between 20 and 100 times [37]. Consequently, it is preferable to perform surface enhancements to turbulators.

The synopsis provided above showed where the PTC's energy efficiency may be improved by using surface modification. Using corrugated tubes was a particular type of surface enhancement for the receiver pipe. When compared to ordinary tubes, corrugated tubing can transport heat more effectively. More surfaces for touching and mixed fluid near the boundary and that flow's center may be connected to this.

Received: July 22, 2025

International Journal of Applied Mathematics
Volume 38 No. 3s, 2025
ISSN: 1311-1728 (printed version); ISSN: 1314-8060 (on-line version)

Additionally, this study's primary goal is to find out how the PTC's thermal efficiency is affected by the helically curved absorber tube according to variable heat flux conditions. There weren't many surveys of the PTC that utilize the spirally corrugated absorbing tube. The effects of the wavy tubes' pitch dimension and roughness amplitude upon the PTC's thermal efficiency were investigated. Additionally, correlations between the Re, sharpness proportion to height, pitching ratio, and changes in the Nu, as well as the f, have been provided.

Numerical methodology

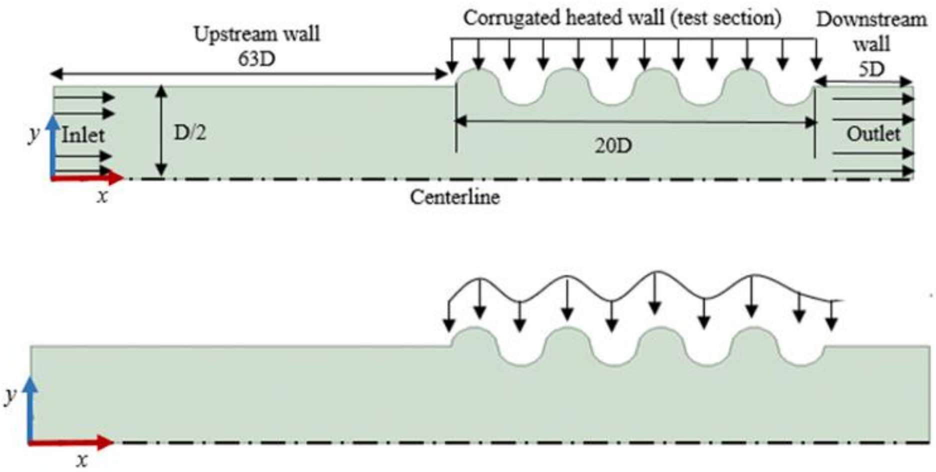

Figure 1 shows the axisymmetric 2-dimensional (2D) flow distribution regarding a circular wavy tube within the axial-radial direction. Moving across the x-direction from upwards to downwards, the flow approaches a steady state. For simplicity, the geometry in Fig. 1(a) hadn't been scaled; instead, it is presented with an enlarged radial expansion.

The tube is 88D in length and has an internal diameter measuring D (8 mm). The flat tube part that makes up the initial 63D part of the intake aids in the development of the airflow. It is followed through a 20D concave segment where UHF as well as NUHF are forced on the exterior of the tube. Near the exit point, the remaining 5D length continues to be straight. The current heat flux patterns utilized in this experiment are shown employing PHF as shown in Figure 1(a).

Boundary conditions

The implemented boundary criteria for the computation zones may be expressed as follows since this study employed 2-dimensional (2D) axisymmetric stream flow:
entry point: $u = ui, v = 0, T = Ti = 303K.$

At walls u=v=0, corrugated wall: assuming the heat flow was identical, a UHF about 1000 W/m2 had been employed. To replicate other varied heat flux variations, especially PHF, thermal fluxes varying between 50 towards 2000 W/m2, administered at intervals of 50 W/m2, have been applied to curvature cavities. in which the number of cavities is C. For PHF, 50 W/m2 heat flux applied on first corrugation cavity then for other cavities Eqn. (3) was used:

$$\mathrm{PHF} = (1051.9\, C^2 - 105.19\, C^2 - 1028.6) \times \sin(-30^\circ) \quad (3)$$

Outlet: $\frac{\partial u}{\partial x} = \frac{\partial v}{\partial x} = 0, P = P_{gauge} = 0.$

Received: July 22, 2025

ISSN: 1311-1728 (printed version); ISSN: 1314-8060 (on-line version)

Governing equations

The following equations represent the continuity, momentum and energy equations for the present cases.

$$\frac{\partial U}{\partial X}+\frac{\partial V}{\partial Y}=0 \tag{4}$$

Momentum (axial and radial directions)

$$U\frac{\partial U}{\partial X}+V\frac{\partial U}{\partial Y}=-\frac{\partial P}{\partial X}+\frac{1}{Re}\left(\frac{\partial^2 U}{\partial Y^2}+\frac{\partial^2 U}{\partial Y^2}\right) \tag{5}$$

$$U\frac{\partial U}{\partial X}+V\frac{\partial U}{\partial Y}=-\frac{\partial P}{\partial Y}+\frac{1}{Re}\left(\frac{\partial^2 V}{\partial X^2}+\frac{\partial^2 V}{\partial Y^2}\right) \tag{6}$$

Energy

$$U\frac{\partial T}{\partial X}+V\frac{\partial T}{\partial Y}=\frac{1}{Re\,Pr}\left(\frac{\partial^2 T}{\partial Y^2}+\frac{\partial^2 T}{\partial Y^2}\right) \tag{7}$$

The dimensionless parameters from the above equations can be expressed as follows:

$$X=\frac{x}{D},\ Y=\frac{y}{D},\ V=\frac{v}{\bar{u}},U=\frac{u}{\bar{u}},\ P=\frac{p}{\rho\bar{u}^2},\ \theta=\frac{T-T_i}{T_w-T_i},\ \Pr=\frac{\mu c_p}{k},\ Re=\frac{\rho\bar{u}D}{\mu}$$

Where

$$X=\frac{x}{D},\ Y=\frac{y}{D},\ V=\frac{v}{\bar{u}},U=\frac{u}{\bar{u}},\ P=\frac{p}{\rho\bar{u}^2},\ \theta=\frac{T-T_i}{T_w-T_i},\ \Pr=\frac{\mu c_p}{k},\ Re=\frac{\rho\bar{u}D}{\mu}$$

Where $\bar{u}$ = average axial velocity at inlet, ρ = fluid density, P = dimensionless pressure, k = thermal conductivity of fluid, μ = dynamic viscosity of fluid, Re = Reynolds number, cp = specific heat of fluid at constant pressure, and Pr = Prandtl number.

The necessary auxiliary equations are as follows:

The average Nusselt number at the tube surface is denoted in Eqn. (8) as follows [15, 19]:

$$\mathrm{Nu}=\frac{\dot{q}D}{(\Delta T)k} \tag{8}$$

where ΔT was the temperature gradient and $\dot{q}$ was the energy flux delivered to the corrugated segment wall. This information is shown in Eqn. (9) as follows [15, 19]:

$$\Delta T=\frac{(T_{wo}-T_o)-(T_{wi}-T_i)}{\ln\left(\frac{T_{wo}-T_o}{T_{wi}-T_i}\right)} \tag{9}$$

Pumping power per unit length, $\dot{W}_p$, is defined in Eqn. (10) as follows [15,19]:

$$\dot{W}_p=\frac{\frac{\pi}{4}D^2\,\bar{u}\Delta p}{L} \tag{10}$$

Where L = length of the tube and Δp = pressure difference.

Received: July 22, 2025

International Journal of Applied Mathematics
Volume 38 No. 3s, 2025
ISSN: 1311-1728 (printed version); ISSN: 1314-8060 (on-line version)

Numerical analysis
ANSYS Fluent v24R1 was used for the computations. The computational fluid domain was divided using a discretization approach into several small cells, and a finite volume model was then put across for simulation purposes. The discretization for the convection components occurred using a second-order upwind method, while the diffusion elements were done using central differencing. In order to create a reliable and effective solution with steady-state flows, the coupled technique was selected as the pressure–velocity linking technique. This solution approach performs better than the others. For simulation purposes, a 2D double-precision implementation was employed. Variables were subjected to a convergence criterion with comparative residuals smaller than 10^{-6}.

Grid independence
To precisely illustrate the boundary layer's behavior, a thin inflation layer has been added, and the quadrilateral-dominant grid approach was used to the whole flow domain, with a particular emphasis on the space around the inner tube wall. Through a typical Re = 500, Figure 2 (a) provides an up-close look at the wire mesh. To further assure precise computational findings, the boundary layer technique inside the mesh region near the cavity wall was used. To improve the weave of the mesh within the wall portion, twenty inflation layers were applied. A methodical mesh refinement research was carried out by progressively reducing the size of each component and tracking the convergence of the average Nu on the surface of the tube to determine the required mesh availability. Both the downstream and upstream curved walls had a maximum of 20 inflation zones applied to them. Fig. 2(b) shows the fluctuation of Nu for various numbers of features. This figure demonstrates that the value of Nu was nearly constant from 260000 elements.

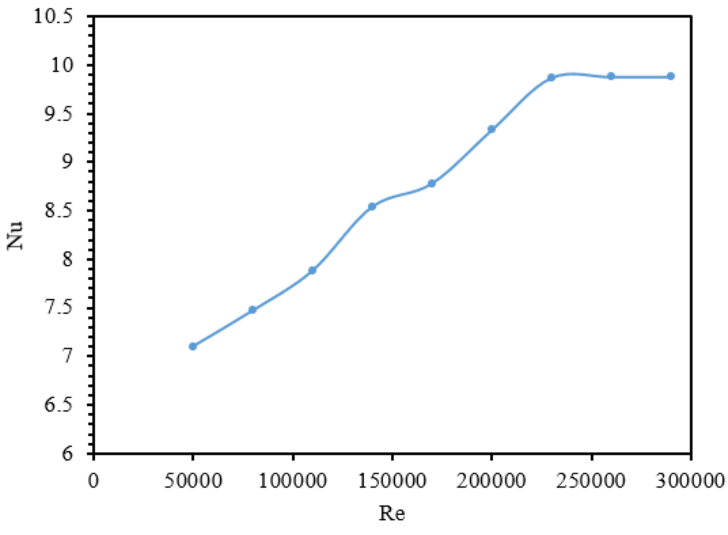

Fig.2 b mesh independence

Results and discussion

This investigation analyzes the thermal-hydraulic characteristics within a semi-circular curved tube during boundary conditions with non-uniform heat flux circumstances involving various Re (500, 600, 700, and 800). Thermal hydraulic effectiveness, enhancement percentages, flow and thermal features, and specific surface Nu variations under various heat flux circumstances are all measured in this study.

Received: July 22, 2025

1. Effect of NUHF on Nusselt number

A heating system's heat transfer efficiency may be evaluated by taking a measurement of the mean Nu over the ribbed tube's face. The average value Nu across all among the four different heat flux concentrations is shown versus Re as shown in Figure 11. Clearly the Re grows, the typical Nu continuously rises, as seen in Fig. 11. According to Newton's Law of Cooling, the reason behind the decrease for the variation in temperature throughout the fluid alongside its surface while Re increases. Furthermore, since the heat flux concentration on the curvature surface varies, Fig. 11 shows that the mean Nu also varies for a given Re. This tendency may be the cause of the higher heat flow in the direction of an outlet within the NUHF state as compared with the UHF, which decreases the slope of the temperature consequently increases the Nu. The lines of trend in Fig. 11 also show a correlation between the mean Nu & Re for the PHF.

2. Effects of NUHF upon power for pumping as well as drag force

As indicated by Fig. 12, the power of the pump and drag force have been calculated as variables based on the Re. they both rise as Re does. Moreover, the surface of the tube is corrugated, increasing surface area and enhancing viscous drag effect. Because there is no change regarding the hydrodynamic boundary states, they are fixed across all wall overheating conditions that are taken into consideration (PHF & UHF). It is also important to note that a larger amount of improvements in heat transfer may be accomplished without experiencing any pumping consumption by using a linearly rising and periodically applied NUHF, which will increase the effectiveness of the energy system.

3. Effect of the NUHF on thermal performance

A NUHF arrangement's ratio with an Nu for UHF , dividing via the NUHF design's average coefficient of friction compared to an UHF installation, is the definition of Thermally Hydraulically Performance (THP). The following [19] is the calculation of the THP factor (η) employing Eqn. (17). A NUHF arrangement's ratio with Nu for UHF Three distinct heat flux situations are shown in relation to UHF as shown in Figure 13(a), where THP parameters are plotted against Re. The change in improvement percent (%) vs Re over the same heat flux situations is also shown simultaneously in Figure 13(b). Figure 13(a) shows that under every heat flux conditions (PHF), the THP stays nearly the same as Re rises. the maximum Re = 600 THP was 1.53.

In regard to Nu improvement percentages, Fig. 13(b) illustrates the enhancement for PHF circumstances relative to UHF. It is noteworthy that, in comparison to UHF, LIHF showed the largest improvement (about 17.81%) around Re = 600.

$$\text{Enhancement percentages} = \frac{Nu_{NUHF} - Nu_{UHF}}{Nu_{UHF}} \times 100\% \tag{19}$$

$$f = \frac{(\Delta p / L)\, D}{(1/2)\, \rho\, \overline{u}^2} \tag{18}$$

Conclusions

A NUHF arrangement's ratio with Nu for UHF Simulation investigation is conducted on the thermally and hydraulically produced properties of circular concave tube in both regular and irregular heated environments. Over the circular ribbed wall surface, uniform (UHF) or non-uniform (PHF) heat fluxes have been used.

1. A NUHF arrangement's ratio with Nu for UHF Simulation investigation is conducted on the thermally and hydraulically produced properties of circular concave tube in both regular and irregular heated environments. Over the circular ribbed

Received: July 22, 2025

ISSN: 1311-1728 (printed version); ISSN: 1314-8060 (on-line version)

wall surface, uniform (UHF) or non-uniform (PHF) heat fluxes since modifications to non-uniform surface heat flux situations do not entail improvements in hydraulic boundary conditions, such non-uniform heat flux circumstances have no effect on streaming functions, velocities vectors, as well as radial motion at the same Re.

2. In comparison to UHF as well as PHF offers higher enhancement, based on the mean Nu.
3. Using trendlines, a straight line between Nu in addition to Re is additionally observed both UHF & PHF.
4. Because there are no variations to the physical boundary conditions at the entrance and exit sections, the power of pumping or drag force with PHF or UHF remain unchanged.
5. Improvement in thermal performance for PHF with 17.8% compared with that for UHF. That means the energy efficiency had been enhancement.

References

1. Khudheyer, A.F., *Optimizing the size for Solar Parabolic Trough Concentrator numerically,* **International Journal of Mechanical Engineering***, 2022, 7(1), pp. 610–615*

2. Khudheyer, A.F, *Turbulent heat transfer for internal flow of ethylene glycol-AL2O3 nanofluid in a spiral grooved tube with twisted tape inserts,* **Journal of Thermal Engineering***, , 7(4), pp. 761–772, 2021*

3. Khudheyer, A.F., *Numerical investigation and exergetic analysis of convergent-divergent absorber tube in concentrated solar trough*, **Journal of Green Engineering**, 2020, 10(10), pp. 8083–8104

4. AL Kareem, S.S.A., Khudheyer, A.F., Mustafa, F.F., *Numerical investigation of turbulent air flow convective heat transfer through a trapezoidal duct*, **Journal of Mechanical Engineering Research and Developments**, 2020, 43(7), pp. 100–108

5. Jebir, S.K., Abbas, N.Y., Khudheyer, A.F., *Effect of different nanofluids on solar radiation absorption*. **Journal of Mechanical Engineering Research and Developments**, 2020, 44(1), pp. 190–206

Received: July 22, 2025